Co-regulation of transcription by BRG1 and BRM, two mutually exclusive SWI/SNF ATPase subunits.

Jesse R. Raab[1], John S. Runge[1,2,3], Camarie C. Spear[1],and Terry Magnuson[1,3]*

Authors Affiliations

1. Department of Genetics, University of North Carolina at Chapel Hill, Chapel Hill, NC 27599, USA

2. Curriculum for Genetics and Molecular Biology, University of North Carolina at Chapel Hill, Chapel Hill, NC 27599, USA

3. Lineberger Comprehensive Cancer Center, University of North Carolina at Chapel Hill, Chapel Hill, NC 27599, USA

* Corresponding Author

Running Title: Cooperative and Antagonistic Transcriptional Regulation by BRG/BRM

Keywords: SWI/SNF, BRG1, BRM, chromatin remodeling, ChIP-seq, RNA-seq, antagonism, cooperativity, transcription

Abstract

Background

SWI/SNF is a large heterogenous multi-subunit chromatin remodeling complex. It consists of multiple sets of mutually exclusive components. Understanding how loss of one sibling of a mutually exclusive pair affects the occupancy and function of the remaining complex is needed to understand how mutations in a particular subunit might affect tumor formation. Recently, we showed that the members of the ARID family of SWI/SNF subunits (ARID1A, ARID1B, and ARID2) had complex transcriptional relationships including both antagonism and cooperativity. However, it remains unknown how loss of a particular subunit affects the binding and genome-wide occupancy of the remainder complex.

Results

We addressed this gap by depleting BRG1, one of the two ATPase subunits in SWI/SNF and characterizing the changes to chromatin occupancy of its sibling subunit BRM. Additionally, we used depletion of BRG1, BRM, or both combined to determine the functional relationship between the two subunits and gene expression. We show that BRG1 loss leads to site-specific gains and losses in BRM occupancy. These differences in BRM occupancy are associated with distinct changes to gene expression. Additionally, we show genome-wide that BRG1 and BRM have both cooperative and antagonistic interactions. Importantly, at genes where BRG1 and BRM antagonise one another we observe a nearly complete rescue of gene expression changes in the combined BRG/BRM double knockdown.

Conclusion

This series of experiments demonstrates that mutually exclusive SWI/SNF complexes have heterogenous functional relationships and highlights the importance of considering the role of the remaining SWI/SNF complexes following loss or depletion of a single subunit.

Introduction

The SWI/SNF complex contains 12-15 subunits [1,2], which are combinatorially assembled to create as many as several thousand biochemically distinct complexes. In development, changes to composition of SWI/SNF can drive developmental progression [3,4]. In cancer, SWI/SNF is among the most commonly found mutations, with mutations observed in as many as 20% of tumors[5,6]. However, these mutations are not equally spread across the subunits. Mutations in the ARID family members (ARID1A, ARID1B, and ARID2) and the ATPase subunits (BRG1 and BRM) are more prevalent than in the other subunits [5,6]. Additionally, in some cancers multiple subunits are mutated. This is the case in hepatocellular carcinoma where mutations have been identified in all three ARID subunits [7–9]. In other cancers, mutations are highly specific, such as BRG1 mutations in Small Cell Carcinoma of the Ovary Hypercalcemic Type (SCCOHT) [10] and SNF5 mutations in malignant rhabdoid tumors [11], and in ARID1A in ovarian clear cell carcinoma [12–14]. The varied relationship between mutations in a particular SWI/SNF subunit and the generation of tumors represents a challenge for determining how the SWI/SNF complex affects transcription and other cellular processes during oncogenesis. Determining how a mutation in one of these subunits affects the remaining subunits of the complex is important for beginning to understand the changes that occur in the mutated state.

We previously used the three ARID subunits as a model to understand how depletion of a single ARID family member affected transcription in a well studied liver cancer line [15]. We showed that the ARID family members had a complex relationship that included both cooperative and antagonistic control of genes. Surprisingly, ARID1B and ARID2 had a highly cooperative effect on gene expression, while ARID1A showed both cooperative and antagonistic effects. Additionally, we showed that all three ARIDs bound a highly overlapping set of regions, but that

differences in the co-factors at subsets of regions might reflect functionally different complexes. However, in that study we did not determine how loss of one of these subunits affected the genomic occupancy of the remaining subunits. It has been shown that SWI/SNF targeting can be affected by a variety of other chromatin regulating families [16,17], including direct competition with PRC1 [18]. Additionally, in synovial sarcoma, the inclusion of an oncogenic fusion protein evicts a core subunit from the complex and leads to retargeting of the remainder complex. However, currently no study has investigated the effect of removing one of the mutually exclusive subunits on the chromatin occupancy of its sibling subunit. Loss of a single member of the complex is the most frequent type of SWI/SNF alteration in cancer, therefore understanding how this affects the remaining complexes function in mechanistic detail is critical.

In this study we examine how loss of one subunit of a mutually exclusive pair affected the localization of its sibling subunit. We conducted an analysis on the two mutually exclusive ATPAse subunits, BRG1 and BRM (also known as SMARCA4 and SMARCA2, respectively). The functional interactions between BRG1 and BRM were not uniform. We show the first genome-wide data for the effect of loss of a mutually exclusive subunit on the remaining sibling. These experiments revealed that a subset of sites bound by BRG1 initially are replaced by BRM binding following BRG1 depletion. A separate subset of sites lost both BRG1 and BRM following BRG1 depletion. Similar to our findings on ARID1A and either ARID1B or ARID2, BRG1 and BRM often antagonize one another in transcriptional control. In cases of antagonism, a combined knockdown of BRG1 and BRM rescued the expression changes globally. These results demonstrate that complex functional interactions exist between mutually exclusive SWI/SNF complexes and highlight the importance of characterizing the effects on the complexes that remain in SWI/SNF mutated tumors.

Results

Comparison of BRG1 and BRM loss in HepG2 cells

We investigated the effect of removing one of the mutually exclusive subunits affected the other sibling subunit using a series of ChIP-seq and RNA-seq experiments following shRNA-mediated knockdown of BRG1 to understand how BRG1 loss affected BRM occupancy and transcriptional regulation. Knockdown of BRG1 using two shRNAs in HepG2 cells has a distinct effect on cell morphology (Fig. 1A, 1B). We then performed ChIP-seq using the stronger shRNA for BRG1. In cells treated with a non-targeting shRNA we observed 28632 BRG1 peaks. Following knockdown this was reduced to 9716 (Fig. 1C). Consistent with that reduction we saw overall BRG1 signal decrease genome-wide approximately 2-fold (Fig. 1 D-F).

We then compared the effect of knockdown of BRG1 to BRM by RNA-seq. shRNA targeting BRG1, BRM, or targeting both BRG and BRM were used to deplete HepG2 of these mutually exclusive subunits and subjected to RNA-seq. The shRNAs selectively targeted the appropriate subunit at the protein (Fig. 2A) and RNA level (Fig. 2B). Consistent with our observations in Figure 1, shBRG1 strongly affected cell morphology by inducing a spindly or mesenchymal morphology compared to the more mounded non-targeting control (Fig. 2C). shRNA targeting BRM also affected cell morphology, however the cells were not spindly and instead appeared more flattened, suggesting BRG1 and BRM do not function identically. The double knockdown was a mixture of the two, although considerably less severe than shBRG1 alone.

We detected many genes that changed following loss of BRG1 (3987), BRM (2775), or the double knockdown (3823) (Fig. 2D, Supplemental Table 1, 2). We used an Upset plot to visualize the overlap between these three groups, separated by the directionality of the gene expression change [19]. This showed that many genes were affected by only one of the shRNAs. This includes approximately 900 genes that were specifically affected by the double knockdown. This group likely includes those where BRG1 and BRM are classically considered redundant.

Next we compared the categories of genes altered by BRG1 and BRM to determine if they affected similar processes. Using the hallmark collection of gene sets from the Molecular Signatures Database [20], we searched for gene sets enriched among the BRG1 or BRM differentially expressed genes. This showed that BRG1 loss lead to an upregulation of genes associated with the epithelial to mesenchymal transition (Fig. 2E) which was consistent with the morphology changes observed, Additionally, BRG1 loss was associated with a decrease in E2F targets and G2M transition genes (Fig. 2E). BRM loss was not significantly negatively associated with any hallmark gene sets. However BRM loss was associated with the upregulation of genes involved in fatty acid and xenobiotic metabolism (Fig. 2E). These results demonstrate that both BRG1 and BRM have numerous effects on gene expression and that their effects are not uniform both at the gene and the pathway level.

BRG1 and BRM occupy similar genomic loci

We next wished to determine how BRM localization is affected following BRG1, therefore we performed ChIP-seq on BRM following knockdown of BRG1 (Supplemental Table 3). Additionally, we mapped changes to H3K27ac to determine how loss of BRG1 on a chromatin

modification associated with active regions of the genome. First, we focused on comparing the relationship between BRG1 and BRM in the normal setting. In the shNS samples the signal for BRG1 and BRM overlapped to a high degree throughout the genome (Fig 3A, B). This is consistent with our previous finding on the ARID subunits and with results on different families of chromatin remodeler that have demonstrated that remodeling complex co-occupy many transcribed genes [15,21]. We identified 18327 sites with peaks of both BRG1 and BRM, and only 9710 BRG1 alone and 4106 BRM alone sites (Fig 3C, p-value < 1e-5 permutation test). The signal at BRG1 only or BRM only was lower than at regions occupied by both BRG1 and BRM (Fig. 3D, E). However, regions that lacked a called peak for one of the subunits did have some signal for the mutually exclusive sibling. This may be due to population effects or represent a lower affinity binding site for the protein.

We next determined how occupancy of BRG1 and BRM were correlated to transcription. Using our expression data from shRNA control cells (Fig. 2) we analyzed the expression of the nearest gene to each ChIP-seq peak separated into three categories (BRG1 + BRM, BRG1 Only, BRM Only). This demonstrated that at the loci occupied by both BRG1 and BRM the associated gene was significantly more highly expressed than genes associated with only BRG1 or BRM (Fig. 3F).

To confirm that the widespread overlap between BRG1 and BRM was not due to lack of specificity of the antibodies we performed immunoprecipitations of BRG1 and BRM using the same antibodies used in ChIP-seq. This showed that each ATPase was purified separately, and could interact with multiple members of the SWI/SNF complex (Fig. 3G). This is consistent with our data from the knockdown experiments (Fig. 2A, B) that also showed that the BRG1 and

BRM antibodies were specific. Together these data suggest BRG1 and BRM primarily bind similar sites genome-wide and when bound together are associated with highly transcribed genes.

Loss of BRG1 causes site-specific loss and gain of BRM

We next analyzed how loss of BRG1 affected the localization of BRM as well as changes to chromatin state. As noted in Figure 1 (same data as Figure 4A) BRG1 depletion led to a robust decrease in the number of peaks called (shNS 28632 compared to shBRG1 9786 Fig. 4A, B, 34% of NS). Similarly, we noted a global decrease in the binding of the active histone mark H3K27ac. The number of H3K27ac peaks were reduced from 43856 in shNS to 21417 in shBRG1 (48% of NS, Fig 4A, B). Nearly all of the BRG1 or H3K27ac peaks retained following knockdown were present in the control cells (2% for BRG1 and 5% for BRM were found in shBRG1 that were not found in shNS). In both cases a small minority of peaks were gained (285 Brg1 peaks, and 1178 H3K27ac peaks), suggesting the predominant effect of BRG1 loss is a decrease in H3K27ac genome-wide. Contrary to the data on BRG1 and H3K27ac occupancy, following BRG1 knockdown we observed both increased and decreased BRM occupancy. 8698 BRM peaks were lost upon BRG1 depletion (38%), 3483 peaks were gained (20%) (Fig. 4A, B). The distribution of genomic features associated with peaks that were altered was consistent across all three antibodies (H3K27ac, BRG1, BRM), as well as between BRM loss and BRM gain sites (Fig 4C). We then looked at where peaks were retained following BRG1 knockdown. BRG1 lost most (~80%) of its non-promoter associated peaks. Similarly, H3K27ac peaks were preferentially retained in the promoter (~75% of peaks remain). This suggested that a basic

level of transcription of some genes is required for continued cell viability and require BRG1 occupancy at promoters.

We next focused on the sites that lose BRG1 (n = 19201, Fig. 5A). Of these sites 1514 gained BRM while 4421 lost BRM (Fig. 5B). The decrease in signal was relatively uniform across all regions measured (Fig. 5B,C). In both the BRM gained and BRM lost category, H3K27ac signal was decreased, however the decrease was more robust at sites losing BRM and BRG1 (Fig. 5C).

We then compared the changes in expression in each of our RNA-seq experiments to the genes closest to the peaks. We compared the fold changes observed following knockdown in each of our conditions for differentially expressed genes associated with our two peak classifications (BRM Gain and BRM Loss). Following loss of BRG1, the expression of genes associated with gains in BRM occupancy significantly increased, while sites associated with BRM loss significantly decreased (Fig. 5D, shBRG1 column). The expression of genes nearest to peaks that gain BRM occupancy significantly decreased expression upon BRM knockdown, while the sites associated with BRM loss were unaffected (Fig. 5D, shBRM column). Finally, when both BRG1 and BRM were knocked down, sites that gain BRM were unaffected, while those that had lost BRM were strongly downregulated. These data suggest a model that at some sites BRG1 and BRM function cooperatively (BRM loss sites), and the loss of BRG1 is the same as losing BRM, while at other sites, they function antagonistically (BRM gain sites). Additionally, this experiment demonstrates that loss of BRG1 has a context specific effect and can lead to either the loss or recruitment of its mutually exclusive partner with changes in gene expression that reflect the differential usage of BRG1 or BRM.

BRG1 and BRM concordant and discordant sites are associated with distinct transcriptional programs.

BRG1 and BRM have previously been shown to antagonize one another in regulating transcription in a developmental context [4], and we have previously shown both antagonistic and cooperative control of transcription by the ARID subunits [15]. Given the high level of co-occupancy genome wide, that BRM occupancy can both increase and decrease following BRG1 loss in a site-specific manner, and that these context specific changes may be indicative of both cooperativity and antagonism between BRG1 and BRM, we next compared the direct role of BRG1 and BRM in transcriptional control. Using the shRNA data described in Figure 2, we analyzed the direction of changes associated with BRG1 and BRM loss at genes that were assigned as the nearest gene to a BRG1 and BRM peak (direct targets). We focused our attention on the 689 genes that were differentially expressed following both BRG1 and BRM knockdown and were the nearest gene to a BRG1 and BRM peak. Comparing all genes affected by either BRG1 or BRM we noted that roughly equal proportions of genes were affected concordantly and discordantly (Fig. 6A). Comparing the fold change of these genes in shBRG1 treated cells to shBRM treated cells revealed that BRG1 and BRM had both cooperative and antagonistic interactions with not good overall correlation (Fig. 6B).

Using the concordance analysis above we assigned each gene to a particular class based on the observed expression changes following BRG1 and BRM loss. This yielded four categories, Both Up (n = 139) , Both Down (n = 164), BRG1 up BRM down (n = 192), BRG down BRM up (n = 194) (Fig. 6A). We then analyzed expression at each of these classes following knockdown by the single or double shRNA. At sites that were regulated concordantly (Both Up or Both

Down), the double knockdown exaggerated the effect slightly, driving expression slightly higher or lower than the single knockdown (Fig. 6C). At genes that were regulated discordantly however there was a robust effect of the double knockdown. In both cases where BRG1 loss upregulated a gene or downregulated a gene and BRM had the opposite effect, the double knockdown strongly blunted these changes returning expression nearly to baseline (Fig. 6C). Therefore, at a large set of genes assayed genome-wide, BRG1 and BRM function antagonistically. We previously observed a similar effect between ARID1A and either ARID1B or ARID2, but at only small number of genes tested individually. These data confirm our previous result and extend it to a new set of mutually exclusive subunits genome wide [15]. These data demonstrate that BRG1 and BRM can have both cooperative and antagonistic effects on gene expression.

Discussion

In this study we show that BRG1 and BRM participate in multiple modes of regulation at both the chromatin occupancy and transcriptional level (Fig. 7). Occupancy of BRG1 and BRM are widespread at active transcription sites and loss of BRG1 can lead to both an increase or decrease in BRM binding in a site-specific manner. Additionally, the changes to transcription are both cooperative and competitive suggesting that regulation by BRG1 and BRM are not governed simply by recruitment. This study highlights the importance of monitoring the effects of remaining SWI/SNF complexes in the context of the loss of one subunit. As this situation occurs commonly in cancer, it is important to consider how the remainder complexes affect transcription and other cellular processes.

Mutually exclusive subunits co-occupy most sites

We and others have previously shown that mutually exclusive members of the same chromatin remodeling family, as well as the ATPase subunits of different families, bind similar sites throughout the genome [15,21]. Here we define similarities in binding profiles between BRG1 and BRM, the two mutually exclusive ATPase subunits of mammalian SWI/SNF. Our data show that the level of occupancy of BRG1/BRM is related to the expression of the gene. Genes where both BRG1 and BRM are bound had the highest levels of transcription (Fig. 3F, Fig. 7). Loss of BRG1 from these sites also lead to the loss of BRM and a decrease in transcription (Fig. 4D, Fig. 7), consistent with a cooperative mechanism of BRG/BRM occupancy at these sites.

Disruption of BRG1 binding has both positive and negative effects on BRG1 occupancy

SWI/SNF is a highly heterogenous complex, consisting of at least seven sets of mutually exclusive subunits as well as several additional subunits such as BAF180 that can be absent or present [1,22]. This complexity allows for the combinatorial assembly of hundreds to thousands of biochemically distinct complexes. Mutations in specific subunits, particularly the ARID subunits and BRG1 are frequent in a variety of tumors [5,6]. However, the complex is commonly studied as one monolithic entity, with disruptions of a single subunit interpreted as disruption of all SWI/SNF function. The number of the complexes that form in a given cell or tumor type, and whether biochemically unique complexes are also functionally distinct is unknown.

A key step in understanding the functional interactions between mutually exclusive subunits is to characterize how loss of one subunit affects the localization of its mutually exclusive partner. In this study, we show that BRG1 loss affects the occupancy of BRM in multiple ways (Fig. 7). There are some sites where loss of BRG1 leads to loss of BRM, suggesting they cooperate or reinforce one another's binding. A second set of regions that lose BRG1 gain BRM and behave

in a classically antagonistic manner in which loss of BRG1 allows BRM to increase occupancy at the region. While this second mechanism has been demonstrated at specific regions before, we show this genome-wide [4,23,24]. Our work highlights that a single mechanism does not exist to explain the functional interaction between two subunits even in a single cell type.

The underlying mechanism that controls how a particular site is regulated remains unclear. One possibility is that each type of occupancy change is associated with specific co-factors or lncRNA that control the outcome following BRG1 loss [25–28]. Analysis of HepG2 ENCODE data at the different classes of BRM occupancy did not show any co-factors or histone modifications selective for a specific subset of peaks (data not shown). A second possibility is that post-translational modifications of SWI/SNF or associated co-factors regulate assembly at these sites. Few studies have looked at these modifications on SWI/SNF, however in breast cancer, methylation of BAF155 by CARM1 is important for SWI/SNF activity in metastatic progression [29]. A final possibility is that the composition of SWI/SNF differs between the different types of sites. Future studies aimed at biochemically purifying subsets of SWI/SNF based on post-translational modifications or genomic loci are needed to determine which mechanisms above are important. However, current methods for purification and identification of the proteins associated with a specific site are limited, making unbiased discovery of the SWI/SNF complexes present or the post-translational modifications difficult at present.

BRG1 and BRM participate in multiple modes of transcriptional regulation

The mechanisms of transcriptional regulation mediated by mutually exclusive subunits of SWI/SNF has previously been grouped into two categories. In one, studies show that BRG1 and BRM are redundant, and the loss of one subunit unmasks a requirement or a new function for the other subunit. This principle underlies the observed synthetic lethality seen between BRG1 and BRM in multiple cancers [30,31]. Similar mechanisms are believed to cause the synthetic lethality observed between ARID1A and ARID1B [32]. Our study provides evidence of this from the large number of genes specifically affected following knockdown of both BRG1 and BRM (Fig. 2D).

A second category of regulatory mechanism is antagonism. In this case the two mutually exclusive subunits have opposing effects on transcription. This has been shown in a developmental context and at specific genes [3,23]. Additionally, we previously observed strong antagonisms between ARID1A and both ARID1B and ARID2 at a subset of genes in HepG2 cells and demonstrated through double knockdown experiments at a small number of genes that the changes in expression observed following knockdown of ARID1A depended on ARID1B and ARID2 [15]. Our expression and occupancy demonstrates that this mechanism is also found in HepG2 cells and is generally applicable to mutually exclusive subunits. Additionally, we see genes where BRG1 plays an activating role in transcription while BRM plays a repressive role. We observe other genes where the reverse is true, suggesting even in a single cell type there is not a consistent functional output to co-occupancy and co-regulation by BRG1 and BRM.

In the current study, we observe a third class where BRG1 and BRM are cooperative. At these genes loss of BRG1 was equivalent to the loss of BRM. These genes were associated with

corresponding changes in occupancy, where loss of BRG1 affects the binding of BRM as well. Peaks associated with highly transcribed genes were often characterized by dual occupancy of BRG1 and BRM, and the loss of either subunit was sufficient to decrease expression of these genes.

As we observed all three types of regulation in a single cell type it suggests that the choices between mechanisms are complex and incompletely understood. Future studies will need to identify the transient interacting partners of SWI/SNF at these distinct classes of sites. Careful dissection of the factors that associate differentially with BRG1 and BRM are required for elucidating how a specific site is targeted by different mechanisms. Our study highlights that SWI/SNF complexes are both biochemically and functionally heterogenous and genome-wide assessments of their role in transcriptional regulation mediated by multiple subunits are needed to gain an accurate picture of their effect in a biological system of interest.

Methods

Cell culture

HepG2 cells were purchased from ATCC. They were grown in DMEM (Gibco, Life Technologies) containing 10% fetal calf serum supplemented with 100units/mL penicillin/streptomycin (Life Technologies). Cells tested negative for mycoplasma contamination and were not passaged more than 6 times from initial cells from ATCC.

Chip-seq

Cells were transduced with shRNA targeting BRG1 or a non-targeting control in the presence of 8ug/mL polybrene. 2ug/mL was added 24 hours post transfection, and cells were grown for a total of 7 days following transduction before harvest. ChIP was performed as previously described with modifications [15]. Cells were fixed for 30 minutes at 4C in 0.3% methanol free formaldehyde, quenched for 5 minutes with 125mM glycine, washed 3 times and snap frozen in liquid nitrogen and stored at -80C. Frozen pellets were thawed for 30 minutes on ice, resuspended each pellet in 1mL swelling buffer (25mM HEPES + 1.5mM MgCl2 + 10mM KCl + 0.1% Igepal containing 1mM PMSF and 1X protease inhibitor cocktail, Roche) and incubated 10 minutes at 4C. Cells were dounced 20 strokes with a “B” pestle and then nuclei were pelleted at 2000 rpm for 7 minutes at 4C. The nuclei were washed with 10mL MNase Digestion Buffer (15mM Hepes pH 7.9, 60mM KCl, 15mM NaCl, 0.32M Sucrose) and pelleted at 2000 rpm for 7 minutes at 4C. The pellet was then resuspended in 1mL MNase Digestion Buffer per 4e7 cells + 3.3uL 1M CaCl2 per mL + PMSF (1mM) and Protease Inhibitor Cocktail (1X, Roche), then incubated for 5 minutes at 37C to warm. We added MNase (NEB M0247S 2000U/ul) at 0.5uL/1e7 cells and incubated for 15 minutes at 37C with agitation. Following digestion, the MNase was chelated using 1/50 volume 0.5M EGTA on ice for 5 minutes. We added 1 volume of 2X IP Buffer (20mM TrisCl pH 8, 200mM NaCl, 1mM EDTA, 0.5mM EGTA), then passed the sample for a 21G needle 5 times and added Triton X-100 to 1% final concentration. The sample was cleared at 13,000 RPM for 15 minutes at 4 degrees and chromatin (30ug BRG1 (abcam

ab110641) /BRM (Cell signaling 11966) or 15ug H3K27ac (active motif 39133)) was used incubated with antibody overnight at 4 degrees. Antibody/chromatin complexes were captured with protein A magnetic beads (Bio-Rad) for 2 hours at 4 degrees, washed 5 times with Agilent RIPA (50mM Hepes pH 7.9/500mM LiCl/1mM EDTA/1% IGEPAL-ca-630/0.7% Na-Deoxycholate) and once with 10mM Tris/1mM EDTA/50mM NaCl. DNA was eluted at 65C with agitation using 100uL 1% SDS + 100mM NaHCO3 made freshly. Crosslinks were reversed overnight by adding 5uL of 5M NaCl and incubating at 65C. DNA was treated with 3uL RNaseA for 30 minutes at 37C and then Proteinase K for 1 hours at 56C and purified with Zymo Clean and Concentrator ChIP Kit and quantified using qubit before library preparation (Kapa Hyperprep).

ChIP-Seq Data Analysis

Mapping

Reads were aligned to hg19 using bowtie2 [33] using the --sensitive parameters, and duplicates were removed using samtools [34]. For visualization bigwig tracks were generated using Deeptools [35] (version 2.2.2) bamCoverage tool with a binsize of 10bp and extending fragments to the approximate nucleosome size of 150bp. Tracks can be visualized using IGV [36] and bw files are available in GEO Accession number GSE102559.

Peak Calling

Peaks were called using Macs2 (version 2.1.0 [37]) using the narrowpeak mode using the following parameters. Qval = 0.001 --keep-dup-all --shift 37 --nomodel --extsize 147. Additionally, we filtered the peaks against the ENCODE blacklist regions and further recursively merged any peaks within 500bp of the nearest peak. Peak calls for each of the six data sets can be found in Supplemental Table 3.

RNA-seq

Cells were transduced with shRNA targeting BRG1, BRM, Both combined, or a non-targeting control in the presence of 8ug/mL polybrene. 24 hours after transduction, 2ug/mL puromycin was added and cells were maintained under selection until harvest (6 days). Cells were

harvested in trizol and RNA was extracted using the Directzol RNA kit (Zymo). Libraries were prepared using the Kapa mRNA library kit per manufacturer's instructions and sequenced on a Hiseq 4000 (50bp).

RNA-seq Data Analysis

Libraries were sequenced on Hiseq 4000 (50bp reads) Gene expression levels were quantitated using kallisto[38]. These data were converted to counts and summarized per gene using tximport [39] and differential expression was carried out using DESeq2[40] using an FDR of 0.05 and no explicit fold change cutoff. Raw count matrices used as input to DESeq2 and output of DESeq2 can be found in Supplemental Tables 1 and 2.

Preparation of Nuclear Lysates

Cells were washed with PBS, then centrifuged at 1300 rpm for 10 min at 4C. Cells were washed with 20 packed cell volumes with hypotonic cell lysis buffer (10mM HEPES-KOH pH 7.9, 1.5mM MgCl2, 10mM KCl, 0.5mM DTT plus protease inhibitors) and placed on ice for 10 min to swell. Cells were then centrifuged at 1300 rpm for 10 min at 4C. Cells were dounced with B pestle in 2 packed cell volumes of hypotonic cell lysis buffer. Nuclei were pelleted at 1300 rpm for 10min at 4C, washed with 10 packed cell volumes with hypotonic cell lysis buffer and centrifuged at 5000 rpm for 10 min. Extractions were performed twice with 0.6 volume nuclear lysis buffer (20mM HEPES-KOH pH 7.9, 25% glycerol, 420 mM KCl, 1.5mM MgCl2, 0.2mM EDTA, 0.5mM and protease inhibitors). Lysates were clarified at 14,000 rpm for 10 min at 4C between extractions. Lysates were diluted with storage buffer (20mM HEPES-KOH pH 7.9, 20% glycerol, 0.2mM EDTA, 0.2mM DTT) to bring final KCl concentration to 150mM and stored at -80.

Immunoaffinity

Prior to beginning the IP, we washed Dynal Protein A beads 3 times with PBS + 0.5% BSA at 4C. We resuspended beads in 400uL of 1X + 0.5% BSA, then added 4-10ug of antibody and incubated overnight at 4C. The following day, we thawed the nuclear lysates on ice. Lysates were added to antibody-conjugated beads and incubated overnight. Beads were washed 4 times with BC-150 (20mM HEPES-KOH pH 7.9, 0.15M KCL, 10% glycerol, 0.2mM EDTA ph 8.0, 0.1% Tween-20, 0.5mM DTT, and protease inhibitors), 2 x BC-100 (20mM HEPES-KOH pH

7.9, 0.1M KCL, 10% glycerol, 0.2mM EDTA ph 8.0, 0.1% Tween-20, 0.5mM DTT, and protease inhibitors), 1 x BC-60 (20mM HEPES-KOH, pH 7.9, 60mM KCl, 10% glycerol, 0.5mM DTT, and protease inhibitors). Proteins were eluted from beads using 2X Laemmli buffer with 100mM DTT for 10 minutes at 95C.

Data Availability

Sequencing from this study is available under the SuperSeries GSE102561 . ChIP-seq data is available in GSE102559. Expression data is available in GSE102560. Processed count matrices for differential expression analysis are contained in Supplemental Table 1. Output for differential expression for the three conditions are found in Supplemental Table 2. Annotated peak calls from ChIP-seq experiments are found in Supplemental Table 3.

1. Clapier CR, Cairns BR. The biology of chromatin remodeling complexes. Annu. Rev. Biochem. 2009;78:273–304.

2. Hargreaves DC, Crabtree GR. ATP-dependent chromatin remodeling: genetics, genomics and mechanisms. Cell Res. Shanghai Institutes for Biological Sciences, Chinese Academy of Sciences; 2011;21:396–420.

3. Lessard J, Wu JI, Ranish JA, Wan M, Winslow MM, Staahl BT, et al. An essential switch in subunit composition of a chromatin remodeling complex during neural development. Neuron. 2007;55:201–15.

4. Flowers S, Nagl NG Jr, Beck GR Jr, Moran E. Antagonistic roles for BRM and BRG1 SWI/SNF complexes in differentiation. J. Biol. Chem. 2009;284:10067–75.

5. Shain AH, Pollack JR. The spectrum of SWI/SNF mutations, ubiquitous in human cancers. Kashanchi F, editor. PLoS One. Public Library of Science; 2013;8:e55119.

6. Kadoch C, Hargreaves DC, Hodges C, Elias L, Ho L, Ranish J, et al. Proteomic and bioinformatic analysis of mammalian SWI/SNF complexes identifies extensive roles in human malignancy. Nat. Genet. 2013;45:592–601.

7. Fujimoto A, Totoki Y, Abe T, Boroevich KA, Hosoda F, Nguyen HH, et al. Whole-genome sequencing of liver cancers identifies etiological influences on mutation patterns and recurrent mutations in chromatin regulators. Nat. Genet. Nature Publishing Group, a division of Macmillan Publishers Limited. All Rights Reserved.; 2012;44:760–4.

8. Guichard C, Amaddeo G, Imbeaud S, Ladeiro Y, Pelletier L, Maad IB, et al. Integrated analysis of somatic mutations and focal copy-number changes identifies key genes and pathways in hepatocellular carcinoma. Nat. Genet. Nature Publishing Group, a division of Macmillan Publishers Limited. All Rights Reserved.; 2012;44:694–8.

9. Li M, Zhao H, Zhang X, Wood LD, Anders RA, Choti MA, et al. Inactivating mutations of the chromatin remodeling gene ARID2 in hepatocellular carcinoma. Nat. Genet. Nature Publishing Group, a division of Macmillan Publishers Limited. All Rights Reserved.; 2011;43:828–9.

10. Le Loarer F, Watson S, Pierron G, de Montpreville VT, Ballet S, Firmin N, et al. SMARCA4 inactivation defines a group of undifferentiated thoracic malignancies transcriptionally related to BAF-deficient sarcomas. Nat. Genet. Nature Publishing Group, a division of Macmillan Publishers Limited. All Rights Reserved.; 2015;47:1200–5.

11. Versteege I, Sévenet N, Lange J, Rousseau-Merck MF, Ambros P, Handgretinger R, et al. Truncating mutations of hSNF5/INI1 in aggressive paediatric cancer. Nature. 1998;394:203–6.

12. Chandler RL, Damrauer JS, Raab JR, Schisler JC, Wilkerson MD, Didion JP, et al. Coexistent ARID1A-PIK3CA mutations promote ovarian clear-cell tumorigenesis through pro-tumorigenic inflammatory cytokine signalling. Nat. Commun. Nature Publishing Group;

2015;6:6118.

13. Jones S, Wang T-L, Shih I-M, Mao T-L, Nakayama K, Roden R, et al. Frequent Mutations of Chromatin Remodeling Gene ARID1A in Ovarian Clear Cell Carcinoma. Science. American Association for the Advancement of Science; 2010;330:228–31.

14. Wiegand KC, Shah SP, Al-Agha OM, Zhao Y, Tse K, Zeng T, et al. ARID1A mutations in endometriosis-associated ovarian carcinomas. N. Engl. J. Med. 2010;363:1532–43.

15. Raab JR, Resnick S, Magnuson T. Genome-Wide Transcriptional Regulation Mediated by Biochemically Distinct SWI/SNF Complexes. PLoS Genet. 2015;11:e1005748.

16. Kim KH, Kim W, Howard TP, Vazquez F, Tsherniak A, Wu JN, et al. SWI/SNF-mutant cancers depend on catalytic and non-catalytic activity of EZH2. Nat. Med. Nature Publishing Group, a division of Macmillan Publishers Limited. All Rights Reserved.; 2015;21:1491–6.

17. Wilson BG, Wang X, Shen X, McKenna ES, Lemieux ME, Cho Y-J, et al. Epigenetic antagonism between polycomb and SWI/SNF complexes during oncogenic transformation. Cancer Cell. 2010;18:316–28.

18. Stanton BZ, Hodges C, Calarco JP, Braun SMG, Ku WL, Kadoch C, et al. Smarca4 ATPase mutations disrupt direct eviction of PRC1 from chromatin. Nat. Genet. [Internet]. Nature Research; 2016 [cited 2016 Dec 12]; Available from: http://dx.doi.org/10.1038/ng.3735

19. Conway JR, Lex A, Gehlenborg N. UpSetR: An R Package For The Visualization Of Intersecting Sets And Their Properties [Internet]. bioRxiv. 2017 [cited 2017 Aug 10]. p. 120600. Available from: http://www.biorxiv.org/content/early/2017/03/25/120600

20. Subramanian A, Tamayo P, Mootha VK, Mukherjee S, Ebert BL, Gillette MA, et al. Gene set enrichment analysis: a knowledge-based approach for interpreting genome-wide expression profiles. Proc. Natl. Acad. Sci. U. S. A. 2005;102:15545–50.

21. Morris SA, Baek S, Sung M-H, John S, Wiench M, Johnson TA, et al. Overlapping chromatin-remodeling systems collaborate genome wide at dynamic chromatin transitions. Nat. Struct. Mol. Biol. Nature Publishing Group, a division of Macmillan Publishers Limited. All Rights Reserved.; 2014;21:73–81.

22. Kadoch C, Crabtree GR. Mammalian SWI/SNF chromatin remodeling complexes and cancer: Mechanistic insights gained from human genomics. Sci Adv. American Association for the Advancement of Science; 2015;1:e1500447.

23. Chandler RL, Brennan J, Schisler JC, Serber D, Patterson C, Magnuson T. ARID1a-DNA interactions are required for promoter occupancy by SWI/SNF. Mol. Cell. Biol. 2013;33:265–80.

24. Mathur R, Alver BH, San Roman AK, Wilson BG, Wang X, Agoston AT, et al. ARID1A loss impairs enhancer-mediated gene regulation and drives colon cancer in mice. Nat. Genet. [Internet]. Nature Research; 2016 [cited 2016 Dec 12]; Available from: http://dx.doi.org/10.1038/ng.3744

25. Zhu P, Wang Y, Wu J, Huang G, Liu B, Ye B, et al. LncBRM initiates YAP1 signalling

activation to drive self-renewal of liver cancer stem cells. Nat. Commun. 2016;7:13608.

26. Wang Y, He L, Du Y, Zhu P, Huang G, Luo J, et al. The long noncoding RNA lncTCF7 promotes self-renewal of human liver cancer stem cells through activation of Wnt signaling. Cell Stem Cell. 2015;16:413–25.

27. Marathe HG, Watkins-Chow DE, Weider M, Hoffmann A, Mehta G, Trivedi A, et al. BRG1 interacts with SOX10 to establish the melanocyte lineage and to promote differentiation. Nucleic Acids Res. [Internet]. 2017; Available from: http://dx.doi.org/10.1093/nar/gkx259

28. Park J, Wood MA, Cole MD. BAF53 forms distinct nuclear complexes and functions as a critical c-Myc-interacting nuclear cofactor for oncogenic transformation. Mol. Cell. Biol. 2002;22:1307–16.

29. Wang L, Zhao Z, Meyer MB, Saha S, Yu M, Guo A, et al. CARM1 methylates chromatin remodeling factor BAF155 to enhance tumor progression and metastasis. Cancer Cell. 2014;25:21–36.

30. McDonald ER 3rd, de Weck A, Schlabach MR, Billy E, Mavrakis KJ, Hoffman GR, et al. Project DRIVE: A Compendium of Cancer Dependencies and Synthetic Lethal Relationships Uncovered by Large-Scale, Deep RNAi Screening. Cell. 2017;170:577–92.e10.

31. Wilson BG, Helming KC, Wang X, Kim Y, Vazquez F, Jagani Z, et al. Residual complexes containing SMARCA2 (BRM) underlie the oncogenic drive of SMARCA4 (BRG1) mutation. Mol. Cell. Biol. 2014;34:1136–44.

32. Helming KC, Wang X, Wilson BG, Vazquez F, Haswell JR, Manchester HE, et al. ARID1B is a specific vulnerability in ARID1A-mutant cancers. Nat. Med. Nature Publishing Group, a division of Macmillan Publishers Limited. All Rights Reserved.; 2014;20:251–4.

33. Langmead B, Salzberg SL. Fast gapped-read alignment with Bowtie 2. Nat. Methods. 2012;9:357–9.

34. Li H, Handsaker B, Wysoker A, Fennell T, Ruan J, Homer N, et al. The Sequence Alignment/Map format and SAMtools. Bioinformatics. 2009;25:2078–9.

35. Ramírez F, Ryan DP, Grüning B, Bhardwaj V, Kilpert F, Richter AS, et al. deepTools2: a next generation web server for deep-sequencing data analysis. Nucleic Acids Res. 2016;44:W160–5.

36. Robinson JT, Thorvaldsdóttir H, Winckler W, Guttman M, Lander ES, Getz G, et al. Integrative genomics viewer. Nat. Biotechnol. 2011;29:24–6.

37. Zhang Y, Liu T, Meyer CA, Eeckhoute J, Johnson DS, Bernstein BE, et al. Model-based analysis of ChIP-Seq (MACS). Genome Biol. 2008;9:R137.

38. Bray NL, Pimentel H, Melsted P, Pachter L. Erratum: Near-optimal probabilistic RNA-seq quantification. Nat. Biotechnol. 2016;34:888.

39. Soneson C, Love MI, Robinson MD. Differential analyses for RNA-seq: transcript-level

estimates improve gene-level inferences. F1000Res. 2015;4:1521.

40. Love M, Anders S, Huber W. Differential analysis of count data--the DESeq2 package. Genome Biol. 2014;15:550.

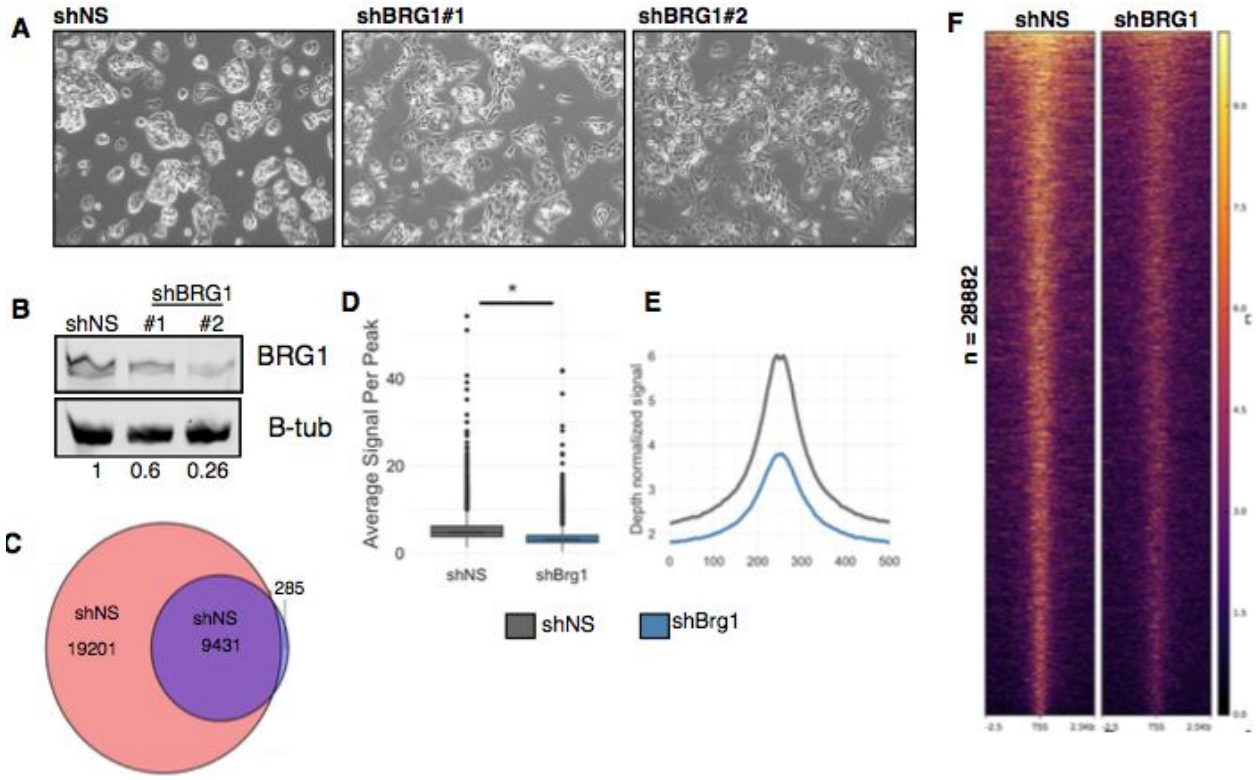

Figure 1: Depletion of BRG1 in HepG2. A. Morphology changes in HepG2 following treatment with 2 shRNAs targeting BRG1. B. Western blot of BRG1 following knockdown. C. Overlap of peaks in cells treated with non-targeting or BRG1 shRNA. D. BRG1 signal at each peak in non-targeting and BRG1 shRNA. E. Metaplot centered on BRG1 peak summits in shNS and shBRG1 HepG2 cells. F. Heatmap of data underlying plots in E.

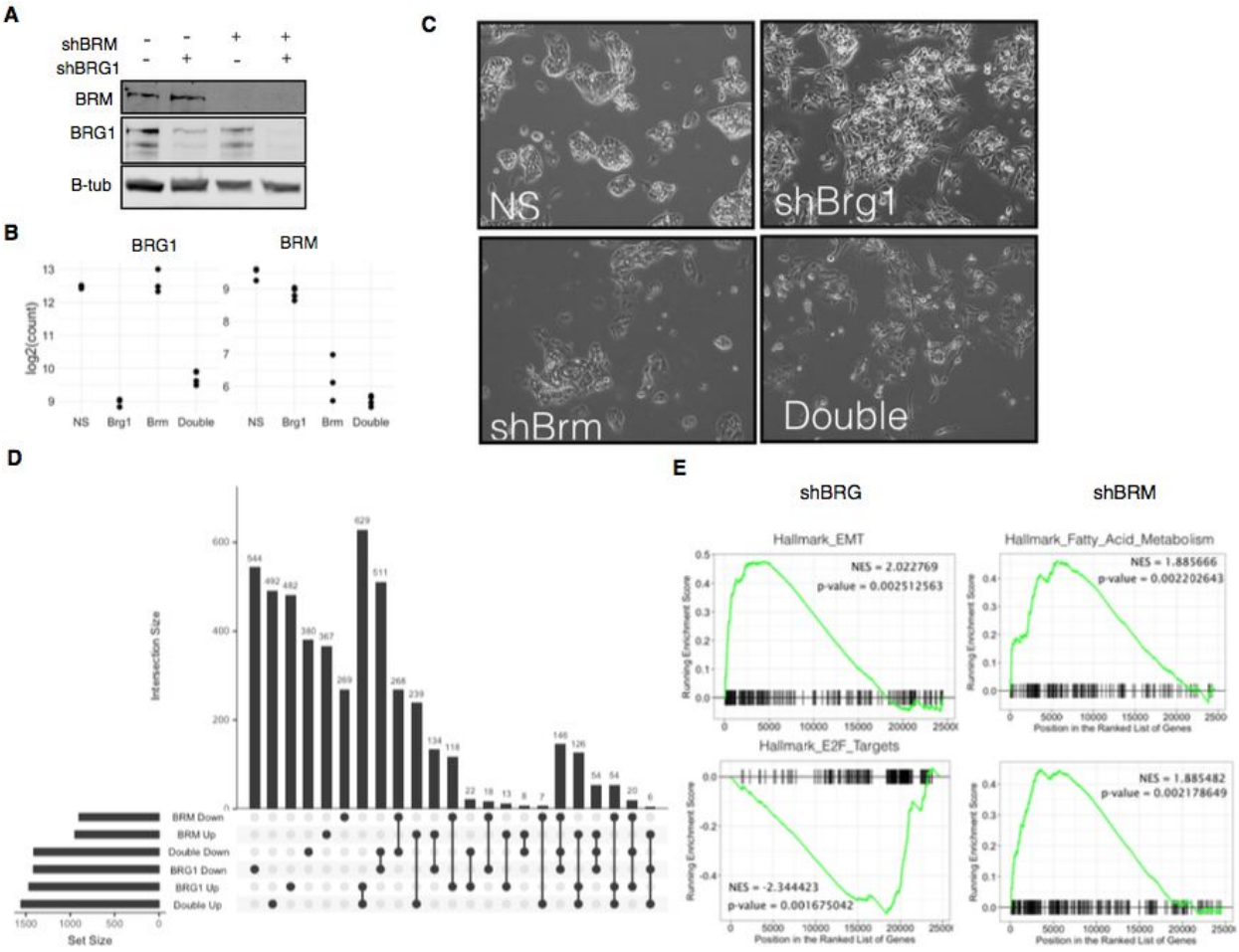

Figure 2: RNA-seq in BRG1, BRM, and combined knockdown. A. Western blot of HepG2 cells treated with shRNA targeting BRG1, BRM, or both combined. B. Log2 normalized read counts of RNA-seq data HepG2 treated with BRG1, BRM or both combined shRNA. C. Morphology changes of shRNA conditions. D. Upset plot showing overlap between genes differentially expressed following shRNA treatment. E. GSEA analysis of shRNA targeting BRG1 and BRM.

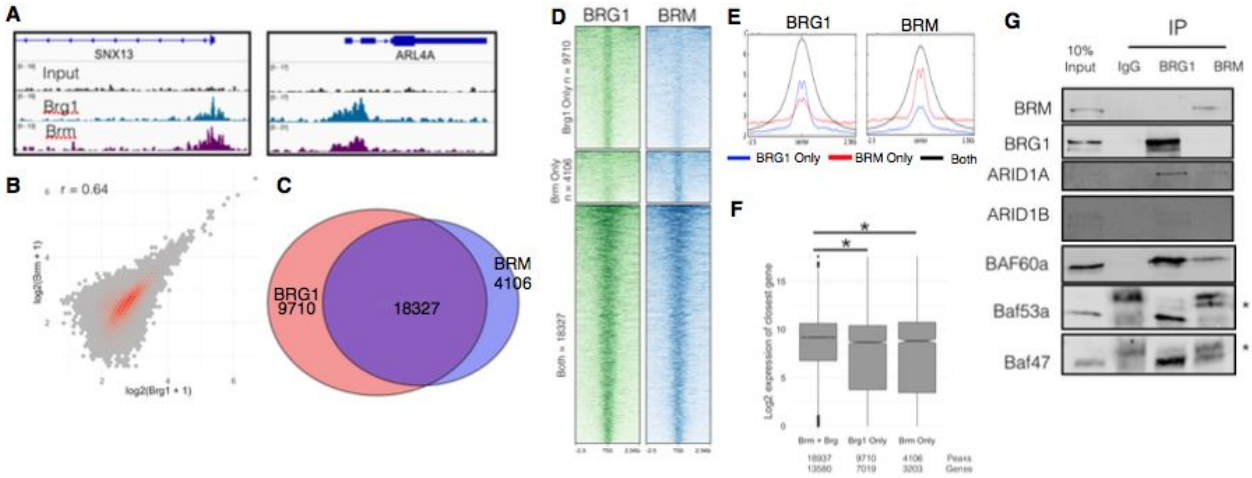

Figure 3: BRG1 and BRM occupy common genomic regions. A. Example of BRG1 and BRM occupancy. B. Scatterplot of signal at union set of BRG1 and BRM peaks. C. Venn diagram depicting overlap between BRG1 and BRM sites. D. Heatmap of signal at BRG1 only, BRM only, BRG1 + BRM peaks. E. Metaplots of signal at three classes of sites. F. Gene expression of nearest gene to three classes of BRG/BRM peaks. Asterisk denotes p-value less than 0.01 G. Co-immunoprecipitation of BRG1 and BRM followed by western blot of SWI/SNF subunits. Asterisks denote IgG heavy chain.

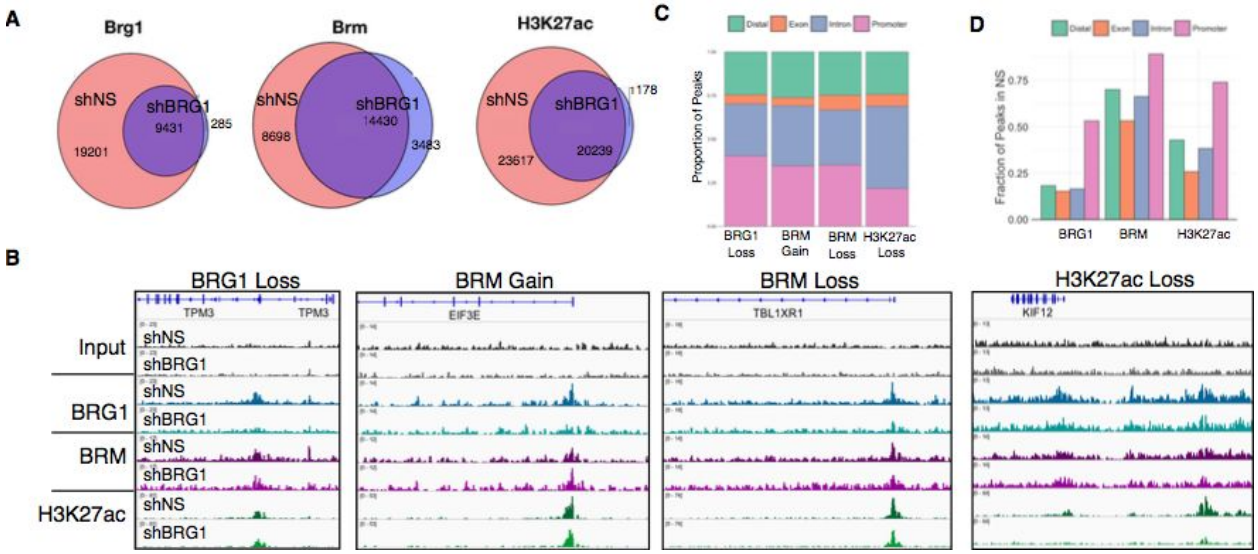

Figure 4: Effect of BRG1 depletion on BRM and H3K27ac binding. A. Venn diagram showing overlap between shNS and shBRG1 for chromatin IPs of BRG, BRM, and H3K27ac. B. Examples of different classes of changes in occupancy following BRG1 depletion. C. Locations of peaks in the different classes. D. The fraction of peaks that are retained following BRG1 depletion assigned to different genomic regions.

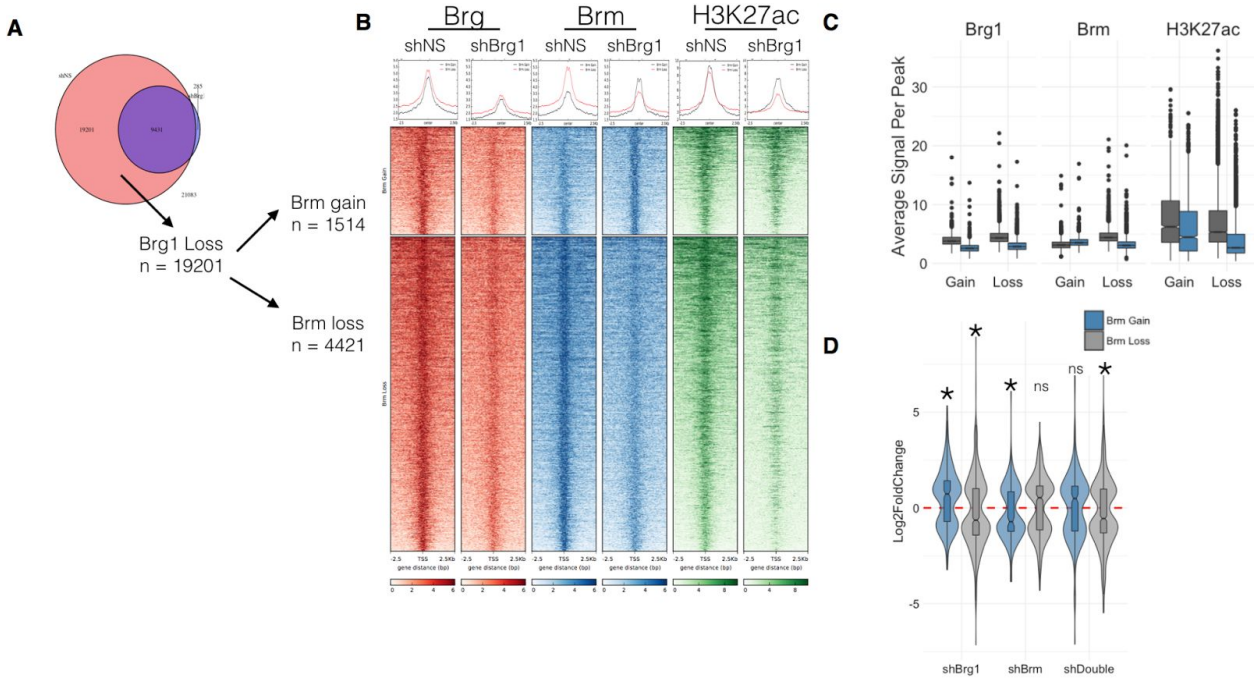

Figure 5 : Occupancy and transcriptional changes associated with BRG1 loss. A. Schematic for selection of peak sets. B. Heatmap of BRG, BRM, and H3K27ac signal at regions that lose BRG1 and either gain or lose BRM. C. Quantification of signal in each category in D. Gene expression changes at significantly changed genes observed following knockdown of BRG1, BRM, or both at BRM gain and BRM loss sites shown as violin plot with boxplot overlaid depicting the 25, 50, and 75 percentiles, asterisk denotes p-values < 0.01 by one-sample wilcox test.

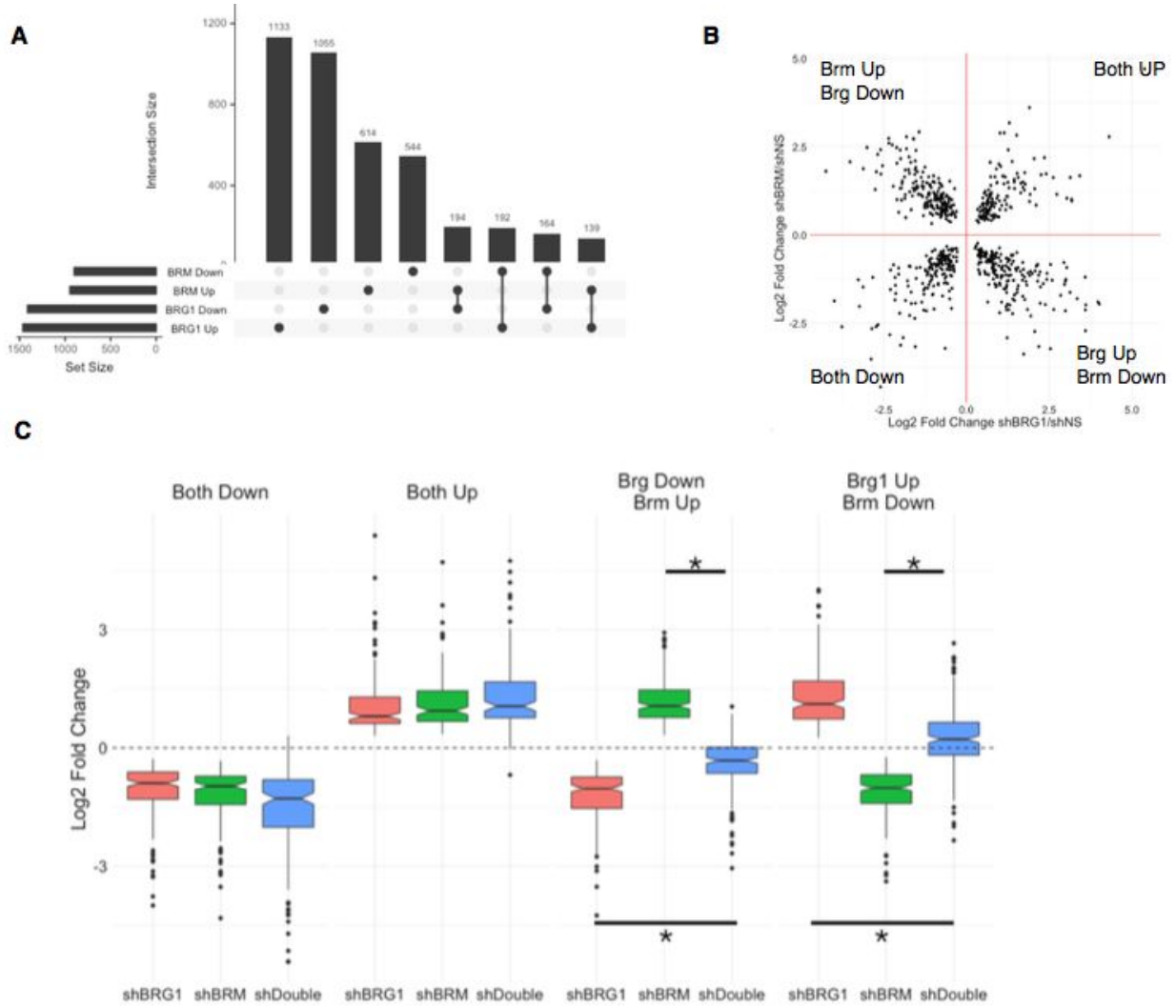

Figure 6: BRG1 and BRM have both cooperative and antagonistic effects on transcription. A. Upset plot showing direction and overlap of differentially expressed genes following BRG1 and BRM knockdown. B Scatterplot of fold changes of the 689 genes that are significantly affected by BRG1 And BRM and are the direct targets of BRG! and/or BRM binding. C. Boxplot of expression changes for the four classes of BRG1/BRM interactions. Asterisks denote p-values < 0.01.

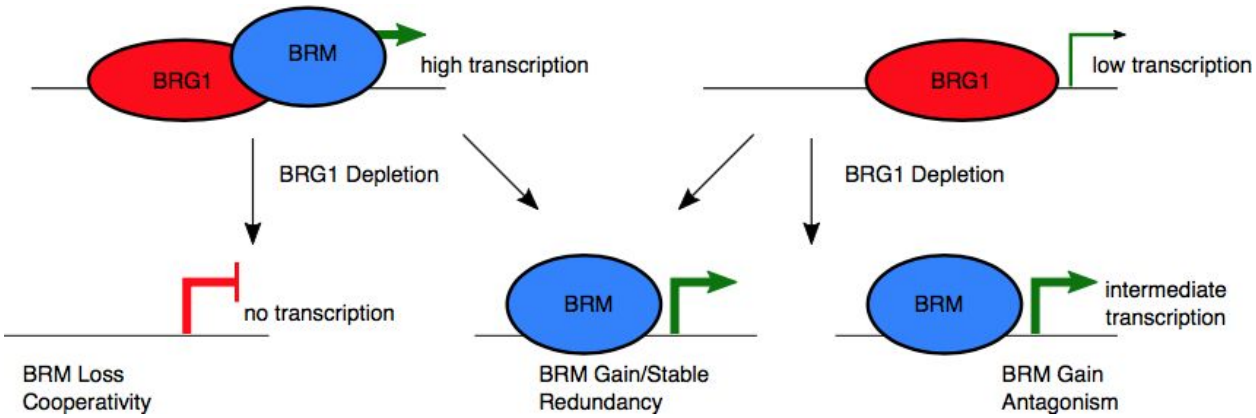

Figure 7: Model for interactions between BRG1 and BRM.